Journal of the European Ceramic Society 21 (2001) 63–70

www.elsevier.com/locate/jeurceramsoc

High temperature mechanical behavior of aluminium titanate–mullite composites

J.J. Meléndez-Martínez [a], M. Jiménez-Melendo [a], A. Domínguez-Rodríguez [a,*], G. Wötting [b]

[a] *Departamento de Física de la Materia Condensada, Universidad de Sevilla, 41080 Seville, Spain*
[b] *CFI, Ceramics for Industry GmbH & Co. KG, D-96472 Rödental, Germany*

Received 6 January 2000; received in revised form 11 May 2000; accepted 26 May 2000

Abstract

Compressive deformation tests at high temperatures (1300–1450°C) have been performed on aluminium titanate (undoped and modified with MgO and Fe_2O_3)–10 wt.% mullite composites obtained by reaction sintering. Two deformation regimes have been observed, depending on the experimental conditions. At high stresses/strain rates, the samples failed intergranularly at very small failure strains. At low stresses/strain rates, large macroscopic strains were reached without significant microstructural changes. MgO and Fe_2O_3 additions have a pronounced effect on the brittle-ductile transition. In contrast, they have no effect on the steady-state flow, which is characterized by a stress exponent close to unity and an activation energy of 650 kJ/mol. Experimental results are compatible with a mechanism of grain boundary sliding controlled by cation bulk diffusion.

Keywords: Al_2TiO_5; Al_2TiO_5-mullite; Creep; Diffusion; Microstructure-final; Mullite

1. Introduction

Aluminium titanate Al_2TiO_5 (AT) ceramics are presently used in automotive industry, thermal processing technology, metallurgy and glass industry because of their low thermal conductivity, low thermal expansion coefficient and excellent thermal shock resistance. Al_2TiO_5 is isomorphous with pseudobrookite, crystallizing in orthorhombic space group Cmcm. This compound is thermodynamically stable from 1280°C to the melting temperature ($T_m = 1860$°C). Below 1280°C, it decomposes into the parent oxides α-Al_2O_3 and TiO_2 by an eutectoid reaction; the decomposition rate is very low below about 800°C.[1] The decomposition can be controlled by adding small amounts of thermal stabilizers, usually MgO and Fe_2O_3, which form complete solid solutions with AT.[2–5]

The mechanical properties of Al_2TiO_5 are strongly determined by its microstructure, which is usually characterized by microcracking. This microcracking phenomenon takes place during cooling from the sintering temperature, owing to the unusually pronounced anisotropy in thermal expansion, thus resulting in poor mechanical properties of the bulk monolithic material. However, a remarkable improvement in room temperature fracture strength over that of pure Al_2TiO_5 has been reported in AT composites containing mullite, Al_2O_3 and/or ZrO_2 as second phases.[6–9] The thermal stability seems to be also favored by the addition of mullite.[6] In a recent work, Liu and Perera[2] have studied the strength and Young's modulus of MgO- and Fe_2O_3-modified AT up to 1200°C. However, nothing is known about the deformation capabilities and mechanisms of AT-based ceramics at elevated temperatures, which is of fundamental importance for their potential high-temperature applications. The objective of the present work was therefore to investigate the high temperature plastic deformation of AT (undoped and modified with MgO and Fe_2O_3)–10 wt.% mullite composites produced by reaction sintering. Mullite second phase was used to reduce the microcracking[7] and eventually improve the creep resistance. The mechanical behavior was evaluated in the temperature range between 1300 and 1450°C by compressive mechanical tests and correlated to the microstructure.

* Corresponding author. Tel.: +34-9-545-57-849; fax: +34-9-546-12-097.
E-mail address: adorod@cica.es (A. Domínguez-Rodríguez).

0955-2219/01/$ - see front matter
PII: S0955-2219(00)00165-5

2. Experimental procedure

Al_2TiO_5 ceramics, supplied by CFI (Ceramics for Industry GmbH & Co. KG, Rödental, Germany) were synthesized by reaction sintering of an equimolar mixture of Al_2O_3 ($d_{50}=0.7$ μm, specific surface area = 7.5 m^2/g and purity = 98.5%) and TiO_2 ($d_{50}=0.5$ μm, specific surface area = 5.5 m^2/g and purity > 98%) powders. The powders were first homogenized with binders by wet ball milling: 10 wt.% mullite ($Al_6Si_2O_{13}$) was incorporated at this stage. After homogenization, green bodies were obtained by slip casting followed by drying and debindering. The resulting green bodies were then sintered at 1460°C in air for 5 h. The materials containing MgO and Fe_2O_3 were prepared in the same way by adding MgO or Fe_2O_3 during ball milling; no residual alumina remained in the sintered materials. After sintering, the density of the three materials (termed undoped AT, Fe–AT and Mg–AT in the following for the sake of brevity) was 3300 kg m^{-3} (~ 90% of the theoretical density).

Rectangular specimens of 4×2×2 mm in size were cut from the as-received materials and mechanically polished finishing with diamond paste of 1 μm-grade. Compression tests were carried out in air at temperatures between 1300 and 1450°C (0.74–0.81 T_m). The deformation experiments were performed: (i) at constant cross-head speed in an Instron universal testing machine, at initial strain rates $\dot{\varepsilon}_o$ between 2×10^{-5} and 4×10^{-4} s^{-1}. The recorded data, load vs. time, were analyzed in σ–ε curves, where σ and ε are the engineering stress and strain, respectively; and (ii) under constant load in a creep machine, at nominal stresses between 2 and 20 MPa. Experimental data, specimen length vs. time, were plotted as log $\dot{\varepsilon}$–ε curves.

The microstructural characterization of the as-received and deformed samples was carried out using scanning electron microscopy (Microscopy Service, University of Sevilla, Spain). To this end, sample sections were mechanically polished and then thermally etched at 1400°C for 45 min in air. The morphological parameters of the various phases were characterized by using a semiautomatic image analyzer. The microstructure of the samples was also examined by transmission electron microscopy (TEM). Thin foils were obtained following a classical procedure of grinding and ion thinning of sliced sections.

3. Results and discussion

3.1. Microstructure of as-received AT ceramics

Fig. 1a is a SEM micrograph illustrating the microstructure of as-received undoped AT. The Al_2TiO_5 grains (bright phase) are almost equiaxed, with an average grain size d (taken as the equivalent planar diameter $d=[4(\text{grain area})/\pi]^{1/2}$) of 4 μm. Mullite grains (dark phase) are rather uniformly dispersed throughout the material, although located preferentially at multiple Al_2TiO_5 grain junctions. Mullite grains have mainly an equiaxed shape, with an average grain size of 1.2 μm, although some grains with acicular shape could also be observed (Fig. 1b). Huang et al.[7] have reported previously these two different morphologies in Al_2TiO_5–25 vol.% mullite composites; the formation of acicular mullite grains was related to the presence of SiO_2-rich regions in their materials. Porosity consisted in relatively large cavities at multiple grain junctions and small ones (diameter < 1 μm) inside the grains (Fig. 1a). Microcracks, both along grain boundaries and in the grains, were also found (Fig. 1a and b), resulting from the highly anisotropic coefficient of thermal expansion of the crystallographic axes. As was mentioned above, the microcracks appears mainly during the cooling of the sintered pieces, although the thermal treatment used to prepare SEM samples may also alter the original microstructure of the as-received samples: during this treatment, the original microcracks may close at about 1000°C and new cracks may form during the cooling. TEM observations showed the presence of very few isolated dislocations inside the Al_2TiO_5 grains. Identical characteristics were found in Mg– and Fe–AT, except

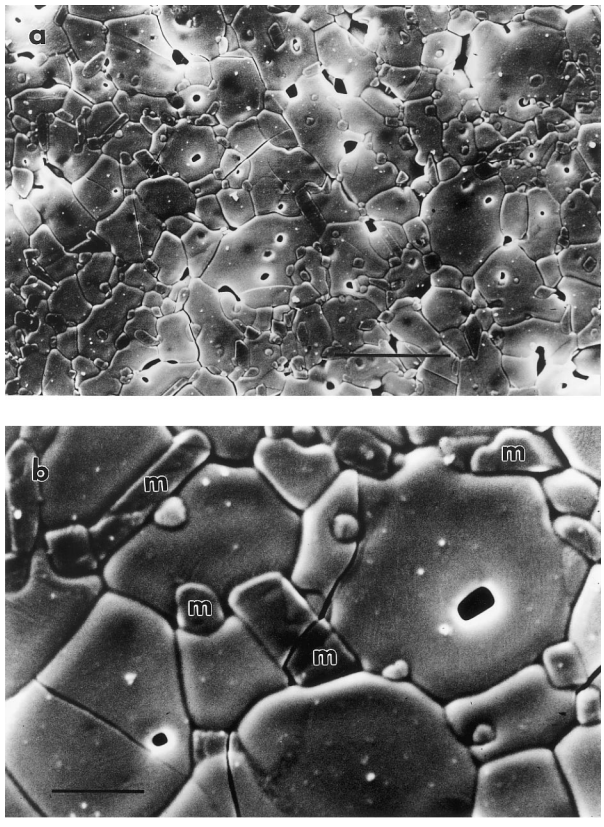

Fig. 1. a. SEM micrograph showing the microstructure of as-received undoped AT (Bar = 10 μm); b. detail of the microstructure of as-received undoped AT. The mullite grains are marked as "m" (bar = 2 μm).

for the larger average grain size of the main Al_2TiO_5 phase, $d = 5.0$ and 5.5 μm, respectively. No evidence of grain-boundary phases could be observed at TEM scale.

The grain size of the Al_2TiO_5 phase is smaller, and microcracking much less severe, than those found in AT ceramics without reinforcing particles obtained at similar sintering conditions.[2,6,8,9] These microstructural features can be attributed to the presence of mullite as second phase, which restrains the grain growth during sintering and simultaneously acts as a hindrance to crack propagation, as can be seen in Fig. 1b. It must be also noted that a decrease in microcracking is concomitant with a reduction in grain size.[10]

3.2. High temperature mechanical behavior

Fig. 2 shows σ–ε curves for undoped, Fe- and Mg-doped AT obtained at 1300 and 1400°C and at an initial strain rate of 4×10^{-5} s^{-1}. For undoped AT, steady-state regimes were established at both temperatures, characterized by an almost constant flow stress. In contrast, catastrophic failure occurred in Fe– and Mg–AT at 1300°C after relatively small strains (about 2%), although the failure was somewhat retarded at 1400°C. Semibrittle fracture was found for undoped AT deformed at an initial strain rate of 4×10^{-4} s^{-1} at 1400°C. Fig. 2 also shows that the peak stress is higher for Fe–AT than for Mg–AT, undoped AT being the softer material, and that the difference in peak stress between the three materials decreases as the ductile behavior is being reached. SEM observations revealed that the fractured surfaces consist completely of intergranular fracture: no intragranular fracture was seen in the samples examined in this study. These results indicate that the strength of the grain boundaries increases with MgO and Fe_2O_3 doping — the small differences in grain size are unable to explain the differences in Fig. 2 — suggesting a segregation of dopant cations to the grain boundaries. Segregation of Mg^{++} ions to grain boundaries has been previously reported by Wohlfromm et al.[8] in 2 wt.% MgO-doped Al_2TiO_5. The importance of dopant segregation to grain boundaries in high-temperature flow stress and ductility of ceramic oxides has been recently realized by Sakuma et al.,[11] who postulated a change in the grain boundary chemical bonding state by the segregation.

In order to extend the investigated stress domain to lower stresses, creep tests at constant load were performed at 1400°C in the three materials. Fig. 3 displays a creep test plotted as log $\dot{\varepsilon}$ vs. ε for undoped AT showing several stress and temperature changes. There are very small transients; the steady-state stage is reached almost immediately upon loading at each stress or temperature change. No evidence of macroscopic failure was found at these low stresses, even after the largest strains studied ($\varepsilon\sim70\%$). Furthermore, the maintenance of the strain rate levels after positive and negative temperature changes (solid lines in Fig. 3) indicates that no grain growth took place during deformation.

The mechanical data have been analyzed using the standard high temperature power law for steady-state deformation:

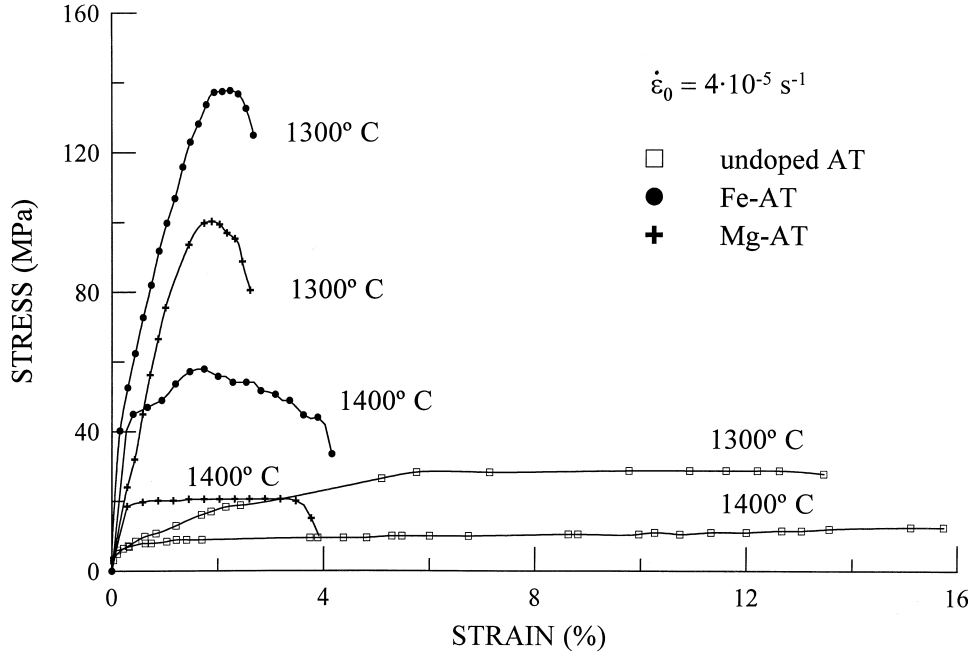

Fig. 2. Engineering stress–strain curves for undoped, Fe- and Mg-doped AT, obtained at 1300 and 1400°C and at an initial strain rate of 4×10^{-5} s^{-1}.

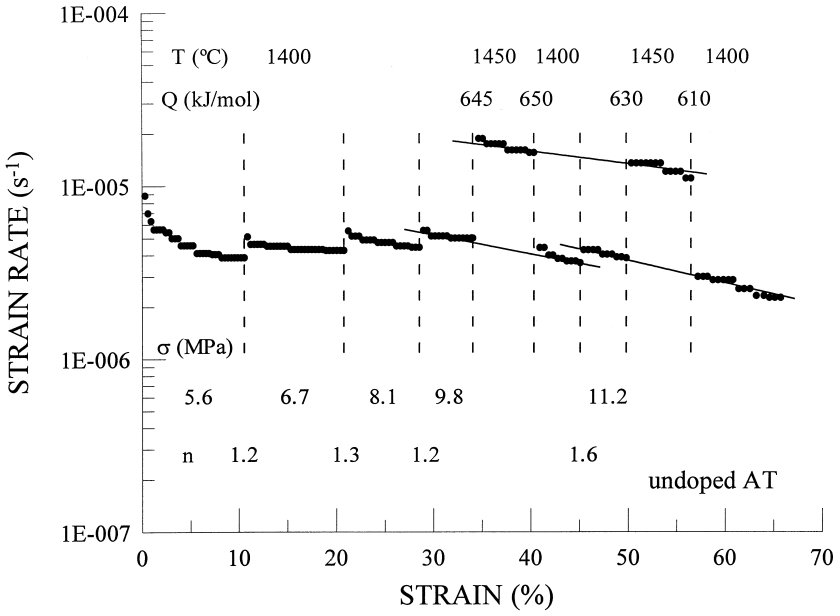

Fig. 3. Creep (log strain rate vs. strain) curve for undoped AT showing several stress and temperature changes to obtain n and Q, respectively.

$$\dot{\varepsilon} = A\sigma^n d^{-p}\exp(-Q/RT) \quad (1)$$

where A is a constant, n the stress exponent, p the grain size exponent and Q the activation energy for flow. Average values of $n=1.3$ (10 determinations) and $Q=650$ kJ/mol (eight determinations) were estimated from Eq. (1) for undoped AT (Fig. 3). Similar results were found in Mg–AT tested under the same experimental conditions, as can be observed in Fig. 4. Although the steady-state strain rate is slightly smaller than that for undoped AT (due to the higher grain size, see below), the same values of the stress exponent and activation energy were found. By contrast, strain rate acceleration — indicative of a progressive failure of the material — was found in Fe–AT at the same experimental conditions shown in Figs. 3 and 4, which is consistent with the limited ductility showed by this material (Fig. 2). However, extensive secondary creep regime ($\varepsilon\sim60\%$) was established in this compound at lower stresses, characterized by the same values of n and Q.

Fig. 5 shows the microstructure of undoped AT under the SEM after steady-state creep up to a final strain

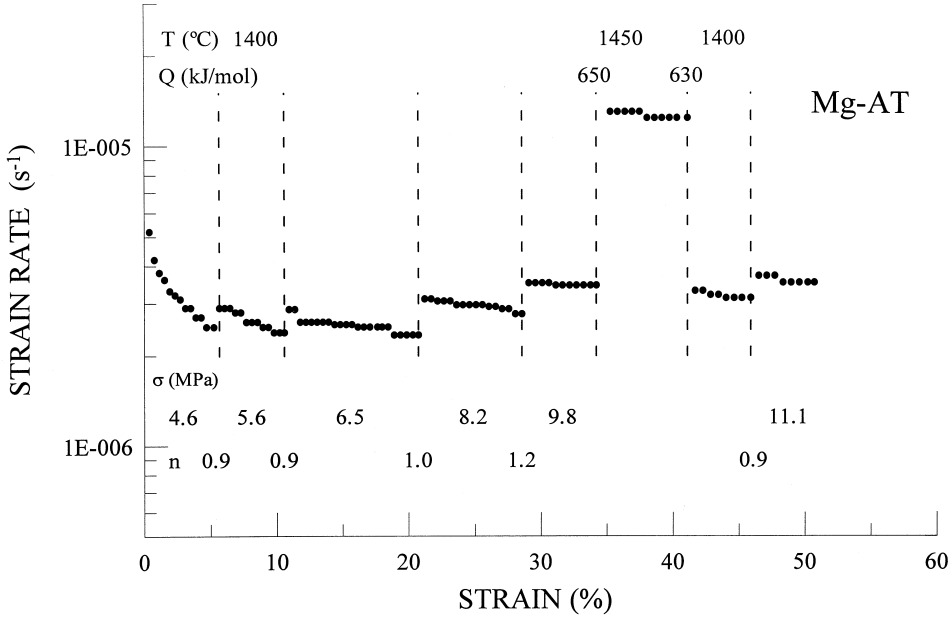

Fig. 4. Creep curve for Mg-doped AT, obtained under conditions close to those for Fig. 3.

$\varepsilon = 0.6$ ($T = 1400°C$, $\sigma = 11$ MPa). Measurements of grain size indicated that no grain growth occurred during deformation, in agreement with what has been noted above from the creep curves. Furthermore, the grains retained their equiaxed shape, with an aspect ratio essentially unaffected by the deformation process. Dislocations were hardly seen in the grains, similar to that observed in the as-received materials, indicating the absence of dislocation activity during deformation. It must be noted that no crack development by cavity or microcrack coalescence is observed, despite the large final strain of the sample ($\varepsilon \sim 60\%$; Fig. 5). Except for the alignment of the needle-like mullite grains perpendicular to the stress axis (arrows in Fig. 5), the same microstructural features are thus exhibited by the as-received and steady-state deformed materials. This result indicates that grain boundary sliding is the primary deformation mechanism at sufficiently low stresses or strain rates.

A stress exponent close to unity has been reported in many ceramic oxides with intermediate grain sizes: Al_2O_3, $n = 1.5$, $d = 3$ μm;[12] NiO, $n = 1.4$, $d = 9$ μm;[13] Y_2O_3-stabilized cubic ZrO_2, $n = 1.4$, $d = 2$–15 μm;[14,15] UO_2, $n = 1.5$, $d = 2$–10 μm;[16] $YBa_2Cu_3O_x$: $n = 1.0$, $d = 10$ μm.[17] In these compounds, the flow process was associated to grain boundary sliding accommodated by diffusion. The value of the stress exponent, together with the absence of both microstructural changes and pronounced transient states in the creep curves (Figs. 3 and 4), suggests that the steady-state deformation of AT ceramics is also provided by the same mechanism. In this case, the strain rate is directly related to the diffusion coefficient D of the slowest-moving species in the compound.[18] To the authors' knowledge, there are no diffusion data for aluminium titanate. However, Freudenberg and Mocellin[19] obtained an apparent activation energy of 700 kJ/mol for the transport of cations across Al_2TiO_5 layers from the growth rate constant for Al_2TiO_5 formation; an effective diffusivity $D = 6.3 \times 10^{-15}$ m^2 s^{-1} for the reaction-rate controlling cation was also estimated by these authors at 1507°C.[20] On the other hand, an activation energy of 615 kJ/mol has been reported in both the creep and the sintering of polycrystalline Ti-doped Al_2O_3.[21] These values are close to that found in our creep experiments ($Q = 650$ kJ/mol), suggesting that bulk cation diffusion is the rate controlling mechanism for grain boundary sliding. Since Ti^{4+} and Al^{3+} occupy the two cationic sites in the Al_2TiO_5 lattice with the same probability and have close ionic radii, it is indeed expected that their activation energies are comparable. A bulk cation diffusion-controlled mechanism is also supported by the following points:

i. Studies by X-ray diffraction[22] and high-resolution transmission electron microscopy[23] have demonstrated a disordered distribution of Al^{3+} and Ti^{4+} ions in the metallic sublattice in Al_2TiO_5; the same situation is encountered in Mg-doped Al_2TiO_5.[23] Because the creation of compensating lattice defects is not required [2 Fe^{3+} ions substitute 2 Al^{3+} in $Fe_{2x}Al_{2(1-x)}TiO_5$, and 1 Mg^{2+} + 1 Ti^{4+} substitute 2 Al^{3+} in $Mg_xAl_{2(1-x)}TiO_5$], it is then expected that the presence of small amounts of dopant cations do not modify significantly the bulk cation diffusion characteristics, yielding the same activation energy for flow. If grain boundary diffusion played an important role, differences in Q would be expected between the three materials because of the segregation of cation dopants to grain boundaries. In ZrO_2-doped Al_2O_3, for instance, the grain boundary diffusivity of Al^{3+} ions has been shown to be greatly reduced with respect to pure Al_2O_3 by the segregation of Zr^{4+} to grain boundaries, increasing the creep activation energy from 500 kJ/mol in pure Al_2O_3 to more than 700 kJ/mol in ZrO_2-doped Al_2O_3.[24,25] The same argument — i.e. segregation of dopant cations to grain boundaries — has been used to explain the lattice diffusion, rather than grain boundary diffusion, control of the superplastic flow in fine-grained Y_2O_3-stabilized ZrO_2 polycrystals.[26]

ii. The Ashby–Verral model for grain boundary sliding accommodated by diffusion[27] has permitted to explain successfully the mechanical behavior observed in other ceramics with similar grain sizes, such as UO_2,[16] NiO,[13] Y_2O_3-stabilized cubic ZrO_2[14] and $YBa_2Cu_3O_x$ superconductor.[17] When lattice diffusion is the rate controlling mechanism, this model leads to:[27]

$$\dot{\varepsilon} = A \frac{\sigma \Omega_{mol}}{kTd^2} D \tag{2}$$

where the constant $A = 98$ and Ω_{mol} is the molecular volume. Using the diffusivity estimated by Freudenberg and Mocellin[20] (corrected at the testing temperature with $Q = 700$ kJ/mol) and $\Omega_{mol} \cong 3 \times 10^{-28}$ m^3,[3] the correlation of Eq. (2) with experimental data is excellent, as shown in Fig. 6. The agreement should be regarded, however, as an estimation within of the order of magnitude, given the simplifying assumptions on

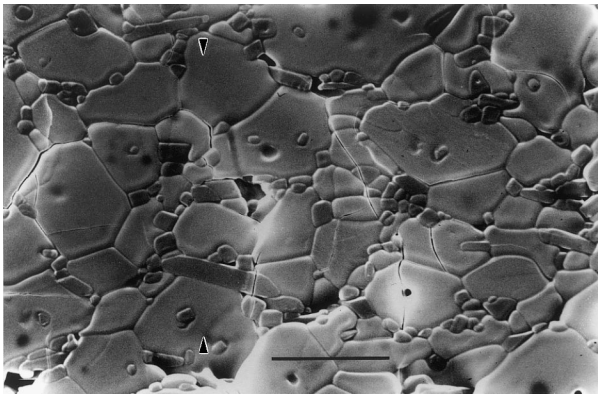

Fig. 5. SEM micrograph showing the microstructure of undoped AT after steady-state creep up to a final strain of 0.6 ($T = 1400°C$, $\sigma = 11$ MPa). The arrows show the compression axis (bar = 10 μm).

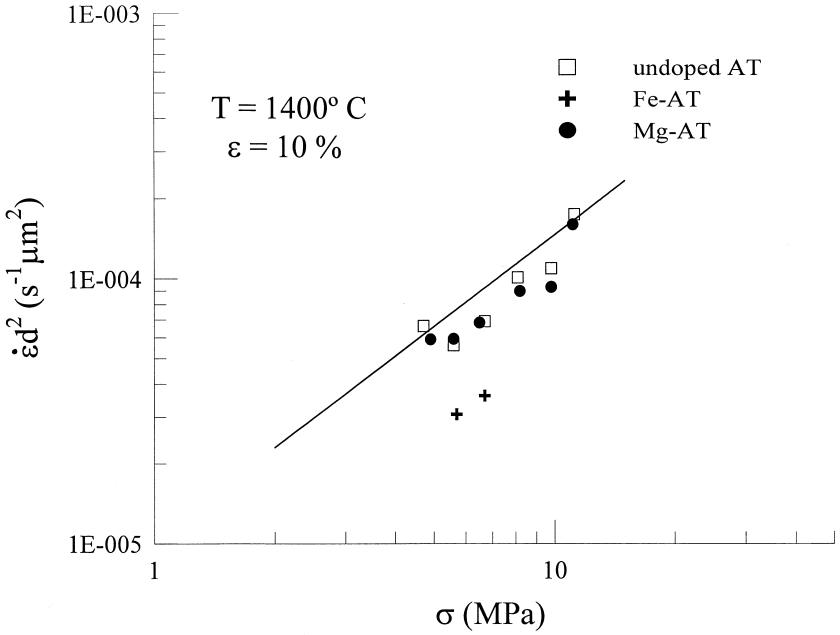

Fig. 6. Grain size-compensated strain rate vs. stress log–log plot for undoped, Fe- and Mg-doped AT ($T=1400°C$, $\varepsilon=10\%$), showing a close agreement with Ashby–Verral model for grain boundary sliding accommodated by diffusion (solid line).

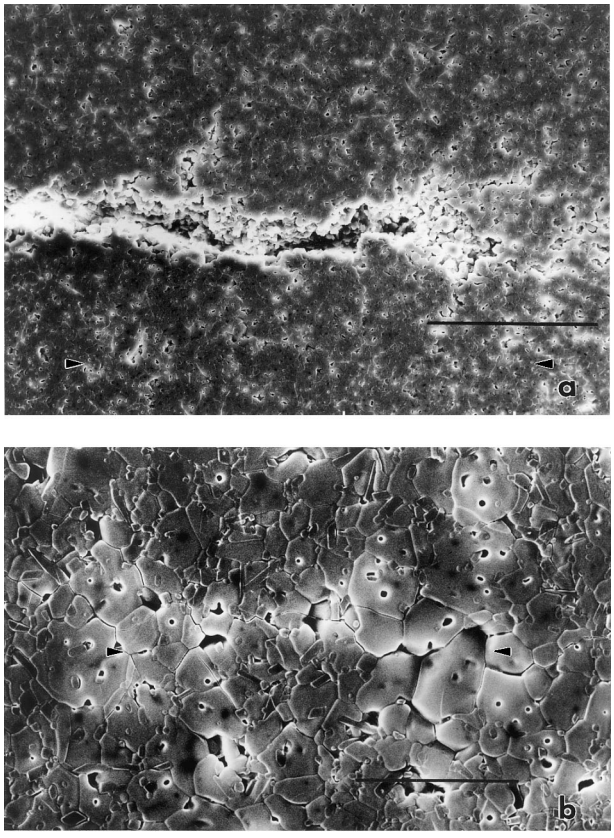

Fig. 7. SEM micrographs showing the microstructure of a sample failed after testing at 1400°C and at an initial strain rate of 4×10^{-4} s^{-1}. The compression axis is marked with arrows: a. single crack producing the failure of the sample (bar = 100 μm); b. coalescence of cavities in two-grain boundaries parallel to the stress direction in regions with large Al_2TiO_5 grains and depleted of mullite grains (bar = 20 μm).

which it is based (the stress exponent is larger than unity, the specimens present a level of porosity able to enhance the deformation rate in a factor 2–3[28] and the cation diffusivity was determined by indirect methods, not by diffusion measurements).

The preceding evidence shows that AT-based ceramics can reach substantial deformation levels without significant microstructural changes when tested at appropriate temperature and stress. Since mullite grains can be considered as rigid particles at these temperature and stress levels — creep rate of polycrystalline mullite with $d=1$ μm is $<10^{-7}$ s^{-1} at 1400°C and 10 MPa[29] — the previous results indicate that this second phase does not increase significantly the creep resistance of Al_2TiO_5. Yoon and Chen[30] have shown that the addition of 10 vol.% mullite to 2 mol% Y_2O_3-stabilized tetragonal ZrO_2 results in a negligible reduction of the creep rate with respect to the monolithic material. These results are also consistent with predictions of a continuum theory for flow of a two-phase composite containing small amounts of rigid and spherical inclusions.[30]

As the stress or the strain rate increases, diffusion can no longer accommodate the sliding of the grains on each other and intergranular cavitation occurs, leading eventually to failure. Fig. 7 shows SEM micrographs of a sample tested at a constant initial strain rate $\dot{\varepsilon}_o=4\times10^{-4}$ s^{-1} at 1400°C and terminated after reaching a peak stress of 30 MPa. The failure of the specimen was due to a single crack developed along the sample, which grew by coalescence of cavities nucleated in two-grain boundaries parallel to the stress direction, indicated

by arrows in Fig. 7a. The cracks are nucleated in large-grained Al_2TiO_5 regions deprived of mullite grains: Fig. 7b shows a magnification of one of these regions close to the main crack. This failure mode has been reported previously in pure alumina at high stresses,[31] where fracture is dictated by the growth of a single crack nucleated at processing flaws (large-grained regions and chemical heterogeneities), with very small failure strains (typically $\sim 1\%$).

4. Conclusions

The mechanical properties of Al_2TiO_5–mullite composites have been studied in compression at constant load and at constant initial strain rate in the temperature range 1300–1450°C. The materials were obtained by reaction sintering of Al_2O_3 and TiO_2 powders with 10 wt.% mullite; samples containing MgO and Fe_2O_3 were also obtained by the same procedure. The materials show a duplex microstructure, consisting of equiaxed and relatively large Al_2TiO_5 grains and small mullite grains located at multiple Al_2TiO_5 grain junctions. Mullite second phase effectively decreases both the final grain size of the main phase and the microcracking inherent to Al_2TiO_5 ceramics.

A brittle–ductile transition has been observed at the present testing conditions. In the brittle regime, intergranular fracture occurs at small strains by the growth of a single crack by coalescence of cavities nucleated at processing flaws. The peak stress is higher in Fe– and Mg–AT than in undoped AT. In the ductile regime, however, large macroscopic strains can be reached without significant microstructural changes, indicating that grain boundary sliding is the primary deformation mechanism in these conditions. The steady-state flow is characterized by a stress exponent close to 1 and an activation energy of 650 kJ/mol in the three materials. Cation bulk diffusion seems to be the strain rate controlling mechanism.

Acknowledgement

This work has been supported by the Brite-Euram project No. BE97-4544.

References

1. Buscaglia, V. and Nanni, P., Decomposition of Al_2TiO_5 and $Al_{2(1-x)}Mg_xTi_{(1+x)}O_5$ ceramics. *J. Am. Ceram. Soc.*, 1998, **81**(10), 2645–2653.
2. Liu, T. S. and Perera, D. S., Long-term thermal stability and mechanical properties of aluminium titanate at 1000–1200°C. *J. Mater. Sci.*, 1998, **33**, 995–1001.
3. Tilloca, G., Thermal stabilization of aluminium titanate and properties of aluminium titanate solid solutions. *J. Mater. Sci.*, 1991, **26**, 2809–2814.
4. Buscaglia, V., Nanni, P., Battilana, G., Aliprandi, G. and Carry, C., Reaction sintering of aluminium titanate: I — effect of MgO addition. *J. Eur. Ceram. Soc.*, 1994, **13**, 411–417.
5. Brown, I. W. M. and McGavin, D. G., Effect of iron oxide additives on Al_2TiO_5 formation. In *Fourth Euro Ceramics*, Vol. 4, ed. A. Bellosi. Faenza Editrice, 1997, pp. 487–492.
6. Lee, H. L., Jeong, J. Y. and Lee, H. M., Preparation of Al_2TiO_5 from alkoxides and the effects of additives on its properties. *J. Mater. Sci.*, 1997, **32**, 5687–5695.
7. Huang, Y. X., Senos, M. R. and Baptista, J. L., Preparation of an aluminium titanate-25 vol.% mullite composite by sintering of gel-coated powders. *J. Eur. Ceram. Soc.*, 1997, **17**, 1239–1246.
8. Wohlfromm, H., Epicier, T., Moya, J. S., Pena, P. and Thomas, G., Microstructural characterization of aluminum titanate-based composite materials. *J. Eur. Ceram. Soc.*, 1991, **7**, 385–396.
9. Zhien, L., Qingmin, Z. and Jianjun, Y., The effects of additives on the properties and structure of hot-pressed aluminium titanate ceramics. *J. Mater. Sci.*, 1996, **31**, 90–94.
10. Ohya, Y. and Nakagawa, Z., Measurement of crack volume due to thermal expansion anisotropy in aluminium titanate ceramics. *J. Mater. Sci.*, 1996, **31**, 1555–1559.
11. Sakuma, T., Ikuhara, Y., Takigawa, Y. and Thavorniti, P., Importance of grain boundary chemistry on the high-temperature plastic flow in oxide ceramics. *Mater. Sci. Eng.*, 1997, **A234–236**, 226–229.
12. Cannon, R. M., Rhodes, W. H. and Heuer, A. H., Plastic deformation of fine-grained alumina (Al_2O_3): I, Interface-controlled diffusional creep. *J. Am. Ceram. Soc.*, 1980, **63**, 46–53.
13. Jiménez-Melendo, M., Domínguez-Rodríguez, A., Márquez, R. and Castaing, J., Diffusional and dislocation creep of NiO polycrystals. *Phil. Magn.*, 1987, **A56**, 767–781.
14. Bravo-León, A., Jiménez-Melendo, M. and Domínguez-Rodríguez, A., Mechanical and microstructural aspects of the high-temperature plastic deformation of yttria-stabilized zirconia polycrystals. *Acta Metall. Mater.*, 1992, **40**, 2717–2726.
15. Dimos, D. and Kohlstedt, D. L., Diffusional creep and kinetic demixing in yttria-stabilized zirconia. *J. Am. Ceram. Soc.*, 1987, **70**, 531–536.
16. Chung, T. E. and Davies, T. J., The low-stress creep of fine-grain uranium dioxide. *Acta Metall.*, 1979, **27**, 627–635.
17. Jiménez-Melendo, M., de Arellano-López, A. R., Domínguez-Rodríguez, A., Goretta, K. C. and Routbort, J. L., Diffusion-controlled plastic deformation of $YBa_2Cu_3O_x$. *Acta Metall. Mater.*, 1995, **43**, 2429–2434.
18. Gordon, R. S., Mass transport in the diffusional creep of ionic solids. *J. Am. Ceram. Soc.*, 1973, **56**, 147–152.
19. Freudenberg, B. and Mocellin, A., Aluminum titanate formation by solid-state reaction of coarse Al_2O_3 and TiO_2 powders. *J. Am. Ceram. Soc.*, 1988, **71**, 22–28.
20. Freudenberg, B. and Mocellin, A., Aluminium titanate formation by solid state reaction of Al_2O_3 and TiO_2 single crystals. *J. Mater. Sci.*, 1990, **25**, 3701–3708.
21. Hollemberg, G. W. and Gordon, R. S., Origin of anomalously high activation energies in sintering and creep of impure refractory oxides. *J. Am. Ceram. Soc.*, 1973, **56**, 109–110.
22. Morosin, B. and Lynch, R. W., Structure studies on Al_2TiO_5 at room temperature and at 600°C. *Acta Crystall.*, 1972, **B28**, 1040–1046.
23. Epicier, T., Thomas, G., Wohlfromm, H. and Moya, J. S., High resolution electron microscopy study of the cationic disorder in Al_2TiO_5. *J. Mater. Res.*, 1991, **6**, 138–145.
24. Wakai, F., Nagano, T. and Iga, T., Hardening in creep of alumina by zirconium segregation at the grain boundary. *J. Am. Ceram. Soc.*, 1997, **80**, 2361–2366.
25. Yoshida, H., Okada, K., Ikuhara, Y. and Sakuma, T., Improvement of high-temperature creep resistance in fine grained Al_2O_3 by Zr^{4+} segregation in grain boundaries. *Phil. Magn. Lett.*, 1997, **6**, 9–14.

26. Jiménez-Melendo, M., Domínguez-Rodríguez, A. and Bravo-León, A., Superplastic flow of fine-grained yttria-stabilized zirconia polycrystals: Constitutive equation and deformation mechanisms. *J. Am. Ceram. Soc.*, 1998, **81**, 2761–2776.
27. Ashby, M. F. and Verrall, R. A., Diffusion-accommodated flow superplasticity. *Acta Metall.*, 1973, **21**, 149–163.
28. Langdon, T. G., Dependence of creep rate on porosity. *J. Am. Ceram. Soc.*, 1972, **55**, 630–631.
29. Ohira, H., Ismail, M. G. M. U., Yamamoto, Y., Akiba, T. and Somiya, S., Mechanical properties of high purity mullite at elevated temperatures. *J. Eur. Ceram. Soc.*, 1996, **16**, 225–229.
30. Yoon, C. K. and Chen, I. W., Superplastic flow of two-phase ceramics containing rigid inclusion-zirconia/mullite composites. *J. Am. Ceram. Soc.*, 1990, **73**, 1555–1565.
31. Wilkinson, D. S., Cáceres, C. H. and Robertson, A. G., Damage and fracture mechanisms during high-temperature creep in hot-pressed alumina. *J. Am. Ceram. Soc.*, 1991, **74**, 922–933.